Title
Inhibition of Photosynthesis by a Fluoroquinolone Antibiotic

Journal
Environmental Science and Technology, 44(4)

ISSN
0013-936X

Authors
Aristilde, Ludmilla
Melis, Anastasios
Sposito, Garrison

Publication Date
2010-02-15

DOI
10.1021/es902665n

Peer reviewed

Environ. Sci. Technol. **2010,** *44,* 1444–1450

Inhibition of Photosynthesis by a Fluoroquinolone Antibiotic

LUDMILLA ARISTILDE,*,† ANASTASIOS MELIS,‡ AND GARRISON SPOSITO†,§

Molecular Toxicology Group, Department of Plant and Microbial Biology, and Division of Ecosystem Sciences, University of California at Berkeley, Berkeley, California 94720

Received September 2, 2009. Revised manuscript received November 30, 2009. Accepted December 7, 2009.

Recent microcosm studies have revealed that fluoroquinolone (FQ) antibiotics can have ecotoxicological impacts on photosynthetic organisms, but little is known about the mechanisms of toxicity. We employed a combination of modeling and experimental techniques to explore how FQs may have these unintended secondary toxic effects. Structure−activity analysis revealed that the quinolone ring and secondary amino group typically present in FQ antibiotics may mediate their action as quinone site inhibitors in photosystem II (PS-II), a key enzyme in photosynthetic electron transport. Follow-up molecular simulations involving nalidixic acid (Naldx), a nonfluorinated quinolone with a demonstrated adverse impact on photosynthesis, and ciprofloxacin (Cipro), the most commonly used FQ antibiotic, showed that both may interfere stereochemically with the catalytic activity of reaction center II (RC-II), the pheophytin−quinone-type center present in PS-II. Naldx can occupy the same binding site as the secondary quinone acceptor (Q_B) in RC-II and interact with amino acid residues required for the enzymatic reduction of Q_B. Cipro binds in a somewhat different manner, suggesting a different mechanism of interference. Fluorescence induction kinetics, a common method of screening for PS-II inhibition, recorded for photoexcited thylakoid membranes isolated from Cipro-exposed spinach chloroplasts, indicated that Cipro interferes with the transfer of energy from excited antenna chlorophyll molecules to the reaction center in RC-II ([Cipro] $\geq$ 5 μM in vitro and $\geq$10 μM in vivo) and thus delays the kinetics of photoreduction of the primary quinone acceptor (Q_A; [Cipro] $\geq$ 0.6 μM in vitro). Spinach plants exposed to Cipro exhibited severe growth inhibition characterized by a decrease in both the synthesis of leaves and growth of the roots ([Cipro] $\geq$ 0.5 μM in vivo). Our results thus demonstrate that Cipro and related FQ antibiotics may interfere with photosynthetic pathways, in addition to causing morphological deformities in higher plants.

Introduction

Fluoroquinolone (FQ) antibiotics, an important class of synthetic antibacterial agents, were developed through structural modifications of the nonfluorinated quinolone nalidixic acid (Naldx; Figure 1A) to act against both Gram-negative and Gram-positive pathogenic bacteria (*1*). Due to this broad-spectrum antibacterial activity, the FQs are widely prescribed in both human and veterinary medicine. However, as a result of incomplete metabolism and the relative ineffectiveness of conventional water treatment technologies in removing them (*2–4*), they are now detected frequently in both receiving and surface waters (*3, 5–7*). Although FQs were developed to have specific mechanisms of action against pathogens through the inhibition of bacterial DNA replication and repair (*1*), they can exhibit unintended toxicological effects on indigenous bacteria and other sensitive organisms when released into the environment (*3, 8–12*). Of special interest are some recent aquatic microcosm studies indicating that photosynthetic species are perturbed when exposed to FQs (*11, 12*). For instance, ciprofloxacin (Cipro; Figure 1B), the dominant FQ antibiotic in current use, has been shown to affect both the structure and richness of algal communities exposed to environmentally relevant concentrations (*11*).

The ability of *Euglena gracilis*, a facultative photosynthetic protozoan, to form green colonies was vitiated as a result of exposure to Naldx (*13, 14*), which also was shown to be a specific inhibitor of chloroplast DNA synthesis. In a key study of seedlings of the higher plant *Arabidopsis thaliana*, grown in media containing Cipro, Wall et al. (*15*) reported that DNA gyrase is a chloroplast-specific enzyme in addition to being a bacterial enzyme, thus revealing a specific target of FQs in photosynthetic organisms that is similar to their bacterial target. The FQs may have other chloroplast-specific targets. For instance, exposure to Naldx led to an inhibition of photosynthetic electron transport (PET) that was an order of magnitude greater than the inhibition of chloroplast DNA synthesis and replication in isolated pea chloroplasts (*16*) and to a reduction in the production of both ATP and NADPH in carrot cell cultures (*17*). These important findings have motivated the proposal (*16*) that Naldx may be acting as a significant inhibitor of photosynthesis, interfering with the generation of reduced electron carriers, which then can impede the production of both ATP and NAD(P)H (*17, 18*). In agreement with the hypothesis of Mills et al. (*16*), in vitro exposure of spinach chloroplasts to nonfluorinated quinolone-containing compounds (*19*) resulted in the inhibition of photosystem II (PS-II) and the cytochrome b_6f complexes, which are key enzymes involved in PET. In sum, these disconcerting results suggest that quinolones, the moieties upon which the broad-spectrum antibacterial activity of FQs largely depends (*1*), may have a toxicological impact on PET similar to that of herbicides (*19*). However, there appear to be no published investigations of the most widely used FQs as to their specific targets in PET.

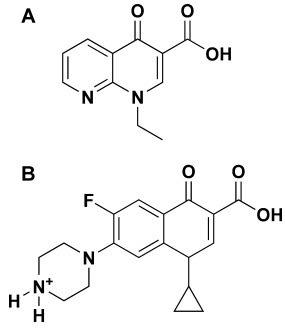

FIGURE 1. Molecular structures of (A) nalidixic acid and (B) ciprofloxacin.

* Corresponding author present address: Department of Geosciences, 158 Guyot Hall, Princeton University, Princeton, NJ 08540; phone: (609) 258-2489; fax: (609) 258-1274; e-mail: ludmilla@princeton.edu.
† Molecular Toxicology Group.
‡ Department of Plant and Microbial Biology.
§ Division of Ecosystem Sciences.

10.1021/es902665n
Published on Web 01/13/2010

In the present study, we employed a combination of modeling and experimental techniques in an effort to probe how FQs may have secondary toxic effects on photosynthetic organisms by interfering with the functioning of PET. We identified the structural components of FQs that may be responsible for photosynthetic inhibition and the possible targeted enzymes by performing a structure−activity relationship (SAR) analysis using well-known protein substrates in and inhibitors of PET. This was followed by molecular modeling of the interactions of Naldx and Cipro with the most likely site of PET inhibition as predicted by the SAR analysis. Guided by these modeling outcomes, we used intact thylakoids isolated from spinach chloroplasts to characterize the effects of Cipro on PET following both in vitro and in vivo exposure at Cipro concentrations up to 50 μM, corresponding to the levels that may be found near industrial effluents (*20*).

Materials and Methods

Materials. Ciprofloxacin (1-cyclopropyl-6-fluoro-4-oxo-7-piperazin-1-ylquinoline-3-carboxylic acid) hydrochloride (>98% purity) was obtained from MP Biomedicals (Solon, OH). All other chemicals were analytical or reagent grade obtained from Sigma-Aldrich.

Modeling FQ Interactions with PS-II. Quinones, and in particular proteins containing quinone sites (Q sites), play an important role in mediating electron transport within the bioenergetic membranes of photosynthetic bacteria, mitochondria, and chloroplasts. To evaluate FQ antibiotics as potential Q site antagonists in PET, 50 known Q site inhibitors which target 8 different proteins involved in photosynthetic and mitochondrial electron transport were subjected to SAR analysis using the LeadScope software package. This software package (*21*) employs a database of molecular structures that are typical in medicinal chemistry to build correlations between important chemical substructures in a selected set of compounds and the biological effects of the compounds. Validation studies of the software to ensure structure−activity correlations specific to each protein target were performed before using it for SAR analysis of the FQs. The principal result of the SAR analysis (for details, see ref *22*) was that four unique chemical substructures (urea, halide aryl, secondary amino group, and 1,4-benzoquinone-2-halo) were identified in about 80% of the compounds that target reaction center II (RC-II), the pheophytin−quinone-type center present in PS-II, wherein photoexcited chlorophyll (Chl) molecules facilitate the flow of electrons from an electron donor chlorophyll to a pheophytin molecule, which then transfers electrons to a primary quinone (Q_A) site (a protein-bound quinone) to reduce subsequently mobile quinone molecules at a secondary quinone (Q_B) site (*20*). Two of the four chemical substructures, namely, secondary amine and halide aryl, are found in the FQ antibiotics pipemidic acid, norfloxacin, enoxacin, lomefloxaicn, and ciprofloxacin. This structural correlation encouraged us to apply molecular docking simulations to explore in more detail the interactions of Naldx and Cipro with the Q_B site in RC-II, a common target of PS-II inhibitors. The quinolone antibiotic Naldx was used for comparison because, as previously noted, it exhibits herbicidal activity by inhibiting PET and possesses fragments of two of the substructures targeting RC-II that are not found in the FQs.

The software package Autodock4 (*23, 24*) was used to generate favorable binding configurations of Naldx and Cipro at RC-II in *Rheudopseudomonas viridis* [PDB ID 2prc (*25*)), which is homologous to RC-II systems found in other photosynthetic organisms (*26*). The docking procedure (*24*) employs a grid map of a three-dimensional lattice (0.2 Å spacing) to store both van der Waals and electrostatic potential energies that would result from the interaction of each atom of the antibiotic ("ligand") with the atoms of the *R. viridis* RC-II ("receptor") located in a specified region considered to be a possible target site of the antibiotic. Accordingly, the L and M subunits of the *R. viridis* RC-II (*25*), which respectively house the binding sites for the protein-bound quinone menaquinone (Q_A) and the soluble quinone ubiquinone (Q_B), were considered in the docking simulations (*22*). A simulation cell having 20 Å sides centered on the Q_B site served to isolate the atoms of the receptor to be included in the grid map. Docking was optimized by allowing the ligand 6 degrees of freedom (rotation and translation) within the cell and by taking into account rotatable bonds of the ligand to include torsional degrees of freedom.

Thermodynamically favorable binding conformations were identified by sequentially implementing random changes in each of the degrees of freedom mentioned above, calculating the intermolecular interaction energies, and subjecting each configuration to an annealing step to remove those that are energetically unfavorable (*22–24*). Visualizations of the lowest energy docking configurations were created using the Maestro software package (*27*). Simulations of the structure of *R. viridis* RC-II cocrystallized with Q_B (Figure 2A) were performed to validate the docking procedure; the conformation of the docked ligand predicted by the simulation was in good agreement with that determined experimentally from crystal structure analysis (*22*). Docking simulations of Naldx and Cipro within the L and M subunits were then performed similarly, with a 20 Å × 20 Å cell centered on the Q_B site; the resulting lowest energy docking realizations were analyzed in detail.

Growth of Spinach Plants. Upon appearance of cotyledons, spinach (*Spinacia oleracea)* seedlings started in 1 in. deep vermiculite pots were grown hydroponically in continuously aerated Hoagland's solution (*28*) in a greenhouse (20 ± 2 °C) under 8 h of daylight. Plants were typically grown to full size in 6−8 weeks.

Isolation of Thylakoid Membranes. Thylakoids were isolated from the spinach leaves (*29*) at 4 °C. Fresh chloroplast isolation buffer solutions (25 mM Tris buffer and 5 mM K_2HPO_4 (pH 7.5), 200 mM sucrose, 10 mM NaCl, 5 mM $MgCl_2$) and thylakoid membrane hypotonic buffer solutions (25 mM Tris buffer and 5 mM K_2HPO_4 (pH 7.5), 10 mM NaCl, 5 mM $MgCl_2$) were prepared daily. Spinach leaves (150 g) in 400 mL of chloroplast buffer solution were blended gradually using a Waring blender until the green tissue of the leaves was entirely in the liquid phase. The resulting slurry was filtered through 16 sheets of cheesecloth and then centrifuged at 500*g* for 2 min. The supernatant solution was centrifuged at 5000*g* for 10 min, and the resulting pellet was resuspended in the chloroplast isolation buffer, homogenized using a tissue homogenizer, and stored in ice until needed. An aliquot of the thylakoid suspension, diluted in 80% acetone and then filtered, was used to quantify the Chl content of the thylakoid suspension via absorbance (*30*). The desired Chl concentration (50 μg of Chl/mL) was obtained by diluting the thylakoid suspension with hypotonic buffer solution prior to the measurements of fluorescence induction during PET.

Fluorescence Induction Measurements. Recording Chl fluorescence induction kinetics (*29*) is a common method of screening for PS-II-inhibiting herbicides (*31, 32*), wherein the shape and rate of the kinetic curves are dependent on the redox state of the electron-accepting protein-bound quinone (Q_A) molecules, which are reduced (to Q_A^-) in the reaction center upon receiving energy from photoexcited Chl (*20*). The shape of these curves is quantified by three parameters (*31*): F_m (the maximum fluorescence intensity following excitation of PS-II, which represents the total amount of Q_A), F_v (the variable fluorescence intensity, representing the amount of Q_A that was photoreduced to Q_A^-), and F_o (the initial fluorescence intensity, which represents the residual amount of Q_A, i.e., Q_A that has not

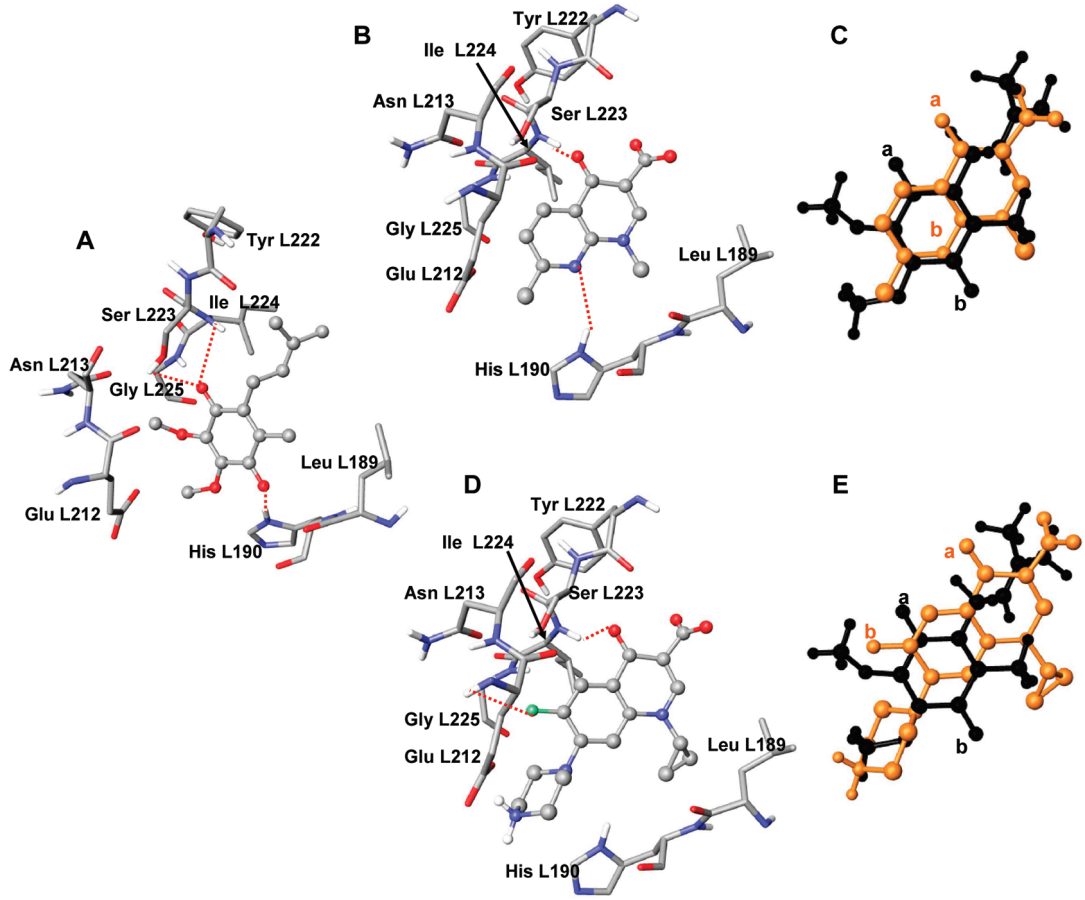

FIGURE 2. Visualizations of molecular docking results for ubiquinone (A, C, E), Naldx (B, C), and Cipro (D, E) in RC-II of *R. viridis*. The amino acid residues in the Q_B binding pocket (A, B, D) are shown in a cylinder motif, while ubiquinone, Naldx, and Cipro are shown in a ball-and-stick motif, and the H-bonds between the amino acids and the docked molecules are shown as dotted lines. In (C) and (E), ubiquinone is shown in black and both Naldx and Cipro are shown in orange (see the text for details). Color legend for the atoms in (A), (B), and (D): O (red), N (blue), F (green), H (white), C (gray).

been photoreduced). Fluorescence induction kinetics were recorded at 690 nm (*33*) after the thylakoid suspensions were treated with 3-(3,4-dichlorophenyl)-1,1-dimethylurea (DCMU), which blocks the reoxidation of Q_A^- by Q_B, to facilitate the accumulation and thus better measurement of Q_A^- (*34*).

In Vitro Exposure. To assess the effects of in vitro exposure to Cipro on PET, the quinone photoreduction process in PS-II was monitored using thylakoid membranes isolated from 4−6 week old spinach plants grown in nutrient solution in the absence of Cipro. Thylakoid suspensions prepared from these plants were exposed to Cipro ([Cipro] = 0, 0.0006, 0.001, 0.1, 0.6, 1, 6, 10, 20, or 50 μM) for 20 or 30 min before their fluorescence induction kinetics were recorded.

In Vivo Exposure. After 8 days following the time of transplantation, spinach plants were transferred into fresh nutrient solutions with [Cipro] = 0, 0.5, 5, or 50 μM. The plants were grown for 26 days before being harvested, after which both the length of the roots and the characteristics of the leaves were assessed. To determine short-term in vivo effects of Cipro on PS-II photochemistry, spinach plants grown 22 days following the time of transplantation were transferred into fresh nutrient solutions that contained [Cipro] = 0, 1, 10, or 50 μM. Thylakoid membranes were isolated from the plants after 8 days of exposure to record their fluorescence induction kinetics using thylakoid suspensions with the same Chl content (50 ± 4 μg/mL).

For both in vitro and in vivo exposures, nominal concentrations of Cipro in solution are reported because there was minimal loss (<10%) to the reaction vessels used in the experiments. For the in vivo experiments, there may be small losses caused by Cipro that is sorbed on the roots but not necessarily taken up by the plant. Both the in vitro and in vivo experiments were carefully replicated.

Statistical Analysis. In each set of replicate experiments, unpaired two-tailed *t* test analyses of the experimental data were performed to assess significant differences between values obtained in the presence of Cipro at several concentrations and data obtained in the absence of Cipro. The concentration−response relationship of the in vivo effects was modeled according to Brain et al. (*35*), where significant differences from the control were determined by subjecting the data to analysis of variance (ANOVA) with subsequent posthoc pairwise comparisons using Dunnett's test as implemented in the SYSTAT statistical computer package (*36*). The lowest concentration with response determined to be significantly different from the control was designated the lowest observable effect concentration (LOEC). Nonlinear regression as implemented in Sigmaplot 9.0 was employed to develop models of significant in vivo effects, from which EC_{50} (the concentration producing a 50% response in the end point as compared to the control) was estimated.

Results and Discussion

Modeling Interactions with Reaction Center II. Both Ile L224 and His L190, two amino acid residues within the L subunit of RC-II, are required to facilitate the binding of Q_B and mediate the enzymatic action of RC-II, i.e., the reduction of bound Q_B (*25*) (Figure 2A). Xenobiotic compounds that react with these and surrounding residues can produce inhibition of PET and the eventual impairment of plant metabolic activity. Many well-known inhibitors of RC-II bind at the Q_B site, notably the herbicide atrazine, which interacts

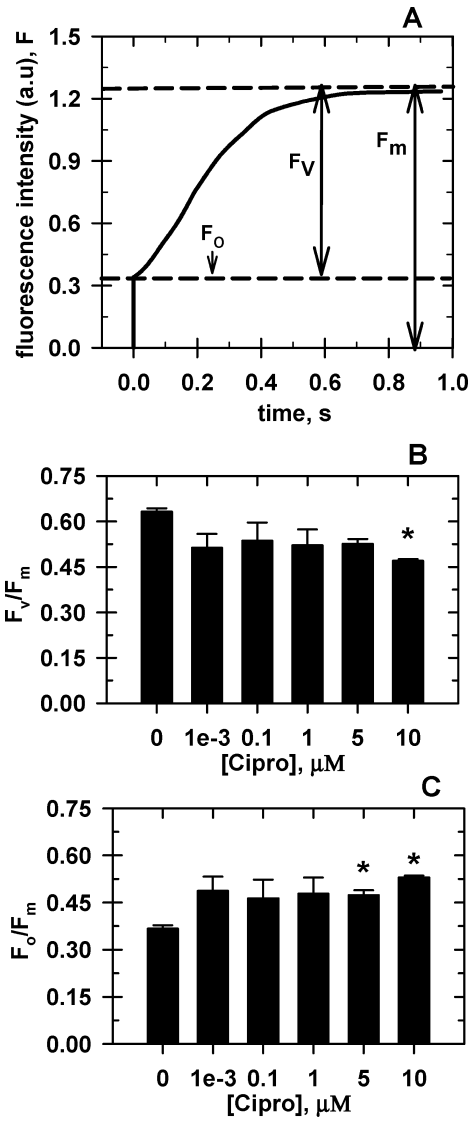

FIGURE 3. (A) Typical fluorescence induction kinetics, showing the relative yield of parameters F_o, F_v, and F_m. Relative measured amounts of F_V (B) and F_o (C) with respect to F_m in spinach thylakoids following 20 min of in vitro exposure to Cipro at several concentrations. Error bars represent standard deviations; $p < 0.03$ (*).

with four residues there, including Gly L225, Ile L224, and, via a bridging water molecule, His L190 (*37*). It is important to note that, while the docking-search target for the antibiotics was situated over a 20 Å × 20 Å grid centered on the Q_B binding pocket, the favorable docking configuration obtained with both Naldx and Cipro was within the specific Q_B binding site (Figure 2), suggesting that the antibiotics have a high affinity for this region of the L subunit. This specific affinity for the Q_B site is in agreement with the outcome of the SAR analysis wherein the quinolone antibiotics were found to possess chemical substructures typical of RC-II Q site inhibitors.

Both the intermolecular H-bonding interactions of each antibiotic with the amino acid residues in the Q_B pocket and the potential interference of the docked antibiotic with the binding of Q_B were examined (Figure 2). The docked Naldx formed two intermolecular H-bonds in the Q_B site: one between the Naldx carbonyl O and Ile L224 and another between its secondary amino group and His L190 (Figure 2B). Comparison of the location of the docked Naldx to that of the bound Q_B (Figure 2C) indicates that Naldx occupies the same binding site as Q_B; i.e., the Naldx carbonyl O (labeled a, in orange) is located near the Q_B carbonyl O (labeled a, in black) that interacts with Ile L224, and the Naldx amino group (labeled b, in orange) is situated near the other carbonyl O in Q_B (labeled b, in black), which interacts with His L190. It was shown previously that exposure of spinach thylakoid membranes to Naldx results in a significant inhibition of O_2 production, a consequence of impaired PET (*16*). We show here, apparently for the first time, specifically how Naldx may bind to the Q_B site of RC-II, including the interactions which may be responsible for the observed inhibition of PS-II by quinolone antibiotics (*18*). By contrast, while the carbonyl O atom from the quinolone ring of Cipro, the prototypical FQ antibiotic, interacts with Ile L224, there was no interaction between Cipro and His L190. Instead, the Cipro F atom forms a H bond with Gly L225 (Figure 2D). Furthermore, comparison of the location of the docked Cipro to that of the bound Q_B (Figure 2E) reveals that Cipro binds in a slightly different region of the Q_B site wherein the Cipro carbonyl O atom (labeled a, in orange) is not as near to the Q_B carbonyl O atom (labeled a, in black) as was the Naldx carbonyl O and the Cipro F atom (labeled b, in orange) was not in the vicinity of the other carbonyl O atom in the Q_B site (labeled b, in black) since, as mentioned above, Cipro did not interfere with the binding of Q_B with His L190. It is important to note that the F atom, in addition to the cyclopropyl and secondary amino groups in Cipro, can be removed as a result of degradation of the antibiotic (*38*) and typical metabolites of Cipro in the environment likely contain only the carbonyl moiety that interacts directly with Ile L224 in RC-II. Therefore, it is conceivable that Cipro may not inhibit PET similarly to Naldx in exposed photosynthetic organisms.

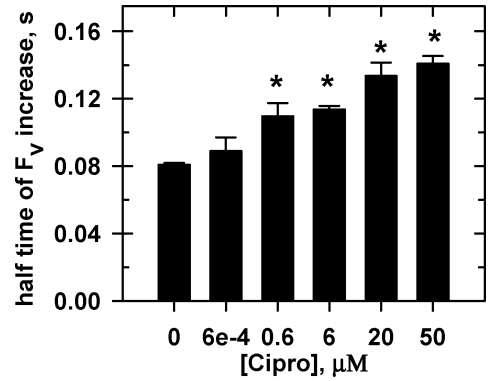

FIGURE 4. Kinetics of photoreduction in spinach thylakoids following 30 min of in vitro exposure to Cipro at several concentrations. Error bars represent standard deviations; $p < 0.05$ (*).

Effects on Photosynthesis. The rate of O_2 production in spinach thylakoids following in vitro exposure to Cipro was not inhibited (*22*), a distinct contrast from previous results obtained with Naldx (*16*), further suggesting that Cipro may have a mode of action different from that of Naldx. This finding is consistent with our modeling results that Cipro may not exhibit a strong binding competition with the secondary quinone (Q_B) at its PS-II target site.

Since Cipro was shown to be structurally similar to known inhibitors of the oxidizing site of PS-II (*22*), which can induce disruption of the redox states required in PS-II for PET, we monitored the redox state of the primary quinone (Q_A) in the presence of Cipro. After in vitro exposure to [Cipro] < 10 μM, there was no statistically significant change in the fraction of Q_A photoreduced, as indicated by the F_v/F_m values (Figure 3B), although an appreciable decrease in F_v/F_m at [Cipro] = 10 μM suggests that Cipro may exert in vitro inhibition of catalytic activity at the Q_A site. Moreover, a statistically significant increase in the F_o/F_m values (Figure 3C) indicates a corresponding increase in the amount of photoexcited Chl

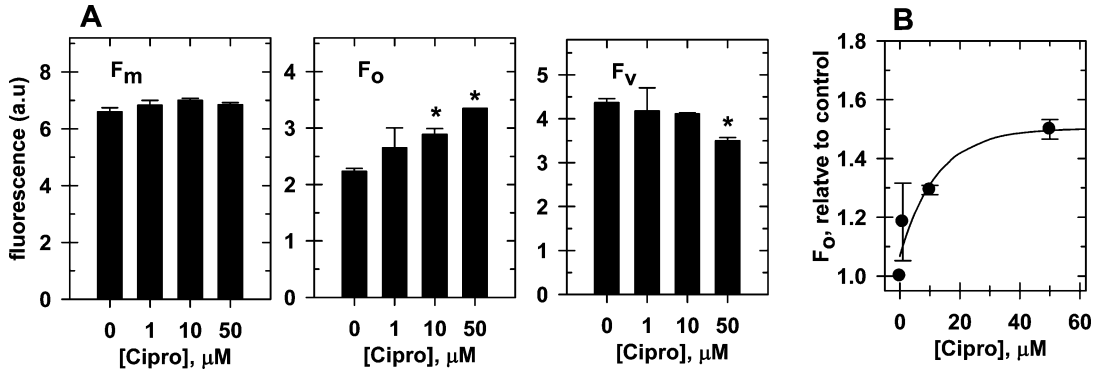

FIGURE 5. Fluorescence induction kinetic parameters as defined in Figure 3 following short-term in vivo exposure of spinach thylakoids to several concentrations of Cipro (A) and F_o relative to the control (2.24 ± 0.05 au) with the calculated response−concentration model for the increase in F_o (B). Error bars represent standard deviations; $p < 0.02$ (*). The line represents the fitted nonlinear regression model obtained with average values of the model coefficients (Table 1).

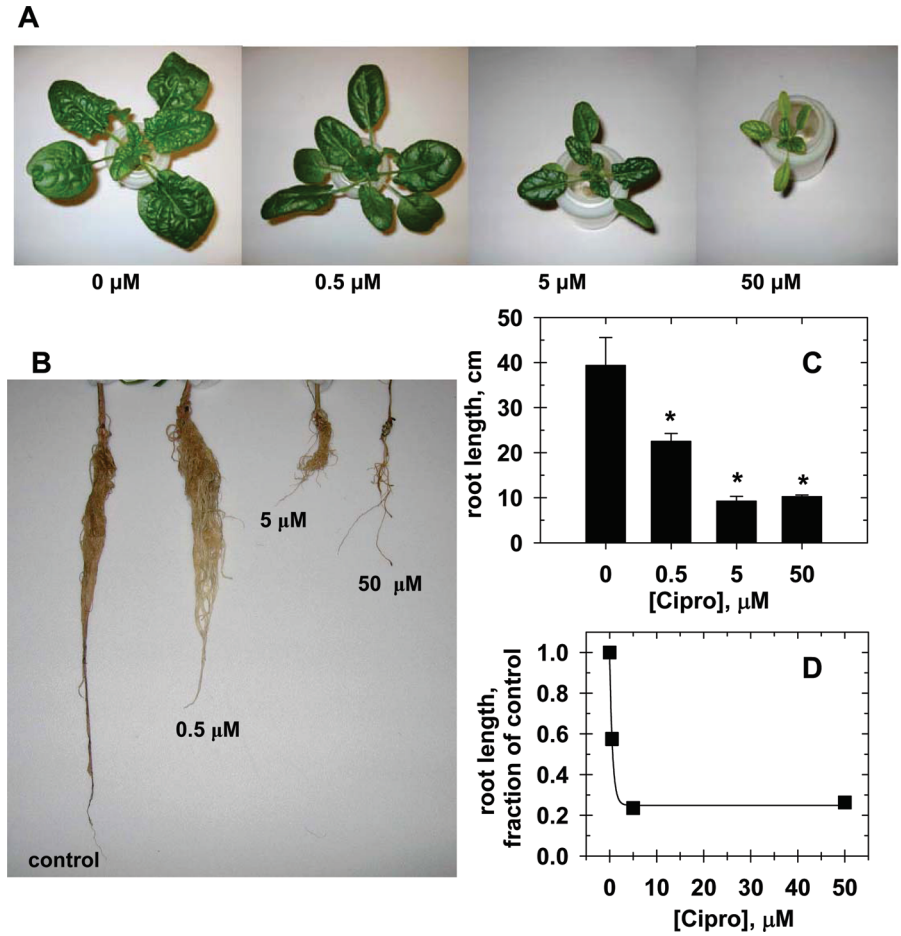

FIGURE 6. Morphological effects of longer term in vivo exposure of spinach plants to Cipro at several concentrations: representative images of leaves (A) and roots (B) of the exposed plants; (C) length of the roots as a function of increasing [Cipro]; (D) length of the roots relative to the control (39.37 ± 6.29 cm) with the calculated response−concentration model for the decrease in the length of the roots. Error bars represent standard deviations; $p < 0.05$ (*). The line represents the fitted nonlinear regression model obtained with average values of the model coefficients (Table 1).

molecules that are not translating to photoreduction of the quinone molecules. In accordance with this phenomenon, the kinetics of Q_A photoreduction were affected significantly as a function of [Cipro] (Figure 4). The calculated time to reach half the maximum value of F_v, i.e., the time to produce half the total amount of photoreduced Q_A, was 0.081 ± 0.001 s in the control experiment, but rose to 0.141 ± 0.004 s at [Cipro] = 50 μM, i.e., a major delay in the kinetics of Q_A photoreduction under our experimental conditions. Taken collectively, these in vitro results led us to propose that Cipro interferes with PET indirectly, by decreasing the rate of energy transfer from antenna Chl molecules to the reaction center in the spinach thylakoids.

The above conclusions were strengthened by results obtained following in vivo exposure of spinach leaves to Cipro. After in vivo exposure, the maximal fluorescence yield (F_m) did not change appreciably, but there were pronounced changes in the relative yields of F_o and F_v (Figure 5). Increasing concentrations of Cipro caused an increase in the parameter F_o, representing the amount of excited Chl that is blocked

TABLE 1. Effective Concentration (EC_{50}, μM) and Lowest Observable Effect Concentration (LOEC) for Two End Points Evaluated Following in Vivo Exposure to Cipro (See the *Materials and Methods*)

end point	response	regression model {exponential: $y_o + a[1 - \exp(-bx)]$}	EC_{50} ($\pm$SE) (μM)	LOEC (μM)	*p* value
inactive PSII chlorophyll units	increase	$y_o = 1.07 \pm 0.05$; $a = 0.435 \pm 0.086$; $b = 0.082 \pm 0.046$ $r^2 = 0.85$	61.0 $\pm$ 50.7	10.0	0.05
root length	decrease	$y_o = -1.00 \pm 0.02$; $a = -0.751 \pm 0.020$; $b = 1.67 \pm 0.14$ $r^2 = 0.99$	0.654 $\pm$ 0.122	0.50	<0.009

from or otherwise incapable of transferring energy to the PSII reaction center (Figure 5). Conversely, the fluorescence parameter F_v decreased systematically with increasing [Cipro] (Figure 5), reflecting the lower levels of excitation energy reaching the PSII reaction center molecule from the antenna chlorophyll. We should point out that this in vivo biochemical effect was observed after a short 8 day exposure to Cipro in the growth media, wherein the plants still appeared to be healthy, with no observable decrease in the green pigment of the leaves, in the amount of newly synthesized leaves, or in the growth of the plant roots. More adverse effects may result from longer exposures.

Following growth of the spinach plants in Cipro-containing nutrient solution for 26 days, we observed stunted growth as evidenced by a significant decrease in the number of newly synthesized leaves and the length of the roots (Figure 6). Similarly, the synthesis of new chloroplasts and mitochondria in both seedlings and cell cultures of *A. thaliana* was severely impaired as a result of exposure to Cipro-containing growth media, with Cipro shown to target DNA gyrase (*15*), just as it does in its antibacterial action. A comparable mechanism may be responsible for the longer term adverse effects of Cipro on the morphology of the spinach plants investigated in the present study; the observable decrease in the amount of both new leaves ([Cipro] $\geq 0.5\,\mu$M) and the green pigment of the leaves ([Cipro] $= 50\,\mu$M) is in agreement with this mechanism (Figure 6A) (*15*).

Both in vitro and in vivo effects of Cipro on Q_A photoreduction underscore that the observed Cipro-induced decrease in the fraction of photoreduced Q_A is not likely due to direct chemical inhibition at the quinone binding site, but instead is a downstream effect of Cipro toxicity in the PS-II units characterized by an increase in inactive antenna Chl molecules. Our experimental results demonstrate that Cipro may interfere with the photosynthetic bioenergetic pathway, in addition to causing morphological deformities in higher plants. The range of EC_{50} values (based on the standard error) estimated from concentration−response models of the increase in inactive excited PSII Chl units (i.e., excited Chl units not involved in mediating quinone photoreduction) and the decrease in root length are, respectively, 10.3−111.7 and 0.532−0.776 μM, both of which are higher than the respective LOEC values (Table 1). Although these concentrations are higher than those typically found in surface waters (*6*), they are comparable with those found near industrial effluents (*20*). Therefore, the observed adverse in vivo response demonstrated here may be relevant to sensitive plants located near high-FQ-containing waters. Finally, the present study not only stresses the need, as pointed out previously (*39*), to consider sublethal molecular targets as potential meaningful phytotoxicity end points, but also takes a step toward the evaluation of FQ cumulative effects, a current challenge in the environmental risk assessment of pharmaceuticals (*35*), by providing correlations between FQ structures and specific molecular mechanisms of toxic action.

Acknowledgments

This research was supported in part by funding from Multistate Research Project W-1082, Evaluating the Physical and Biological Availability of Pesticides and Pharmaceuticals in Agricultural Contexts. We are most grateful to Dr. Dale E. Johnson (Molecular Toxicology Group, University of California at Berkeley) for access to the LeadScope software package and for insightful discussions during the SAR modeling, to Dr. Kathleen A. Durkin (Molecular Graphics and Computation Facility, University of California at Berkeley) for technical assistance with the molecular docking simulations, to John Franklin (College of Natural Resources Greenhouse Facility, University of California at Berkeley) for assistance in the growth and maintenance of the spinach plants, to Andrew Yang for logistical assistance, and to three anonymous reviewers for their insightful comments.

Literature Cited

(1) Brighty, K. E.; Gootz, T. D. In *The Quinolones*, 3rd ed.; Andriole V. T., Ed.; Academic Press: San Diego, CA, 2000; pp 34−98.
(2) Renew, J. E.; Huang, C.-H. Simultaneous determination of fluoroquinolone, sulfonamide, and trimethoprim antibiotics in wastewater using tandem solid phase extraction and liquid chromatography−electrospray mass spectrometery. *J. Chromatogr., A* **2004**, *1042*, 113–121.
(3) Dodd, M. C.; Shah, A. D.; von Gunten, U.; Huang, C.-H. Interactions of fluoroquinolone antibacterial agents with chlorine: Reaction kinetics, mechanisms, and transformation pathways. *Environ. Sci. Technol.* **2005**, *39*, 7065–7076.
(4) Dewitte, B.; Dewulf, J.; Demeestere, K.; van de Vyvere, V.; de Wispelaere, P.; van Langenhove, H. Ozonation of ciprofloxacin in water: HRMS identification of reaction products and pathways. *Environ. Sci. Technol.* **2008**, *42*, 4889–4895.
(5) Golet, E. M.; Alder, A. C.; Giger, W. Environmental exposure and risk assessment of fluoroquinolone antibacterial agents in wastewater and river water of the Glatt Valley watershed, Switzerland. *Environ. Sci. Technol.* **2002**, *36*, 3645–3651.
(6) Kolpin, D. W.; Furlong, E. T.; Meye, M. T.; Thurman, E. M.; Zaugg, S. D.; Barber, L. B.; Buxton, H. T. Pharmaceuticals, hormones, and other organic wastewater contaminants in U.S. streams 1999−2000: A national reconnaissance. *Environ. Sci. Technol.* **2002**, *36*, 1202–1211.
(7) Lindberg, R. H.; Wennberg, P.; Johansson, M. J.; Andersson, B. A. V. Screening of human antibiotic substances and determination of weekly mass flows in five sewage treatment plants in Sweden. *Environ. Sci. Technol.* **2005**, *39*, 3021–3029.
(8) Cordovas-Kreylos, A. L.; Scow, K. M. Effects of ciprofloxacin on salt marsh sediment on microbial communities. *ISME J.* **2007**, *1*, 585–595.
(9) Halling-Sorensen, B. Inhibition of aerobic growth and nitrification of bacteria in sewage sludge by antibacterial agents. *Arch. Environ. Contam. Toxicol.* **2001**, *40*, 451–460.
(10) Lewis, K. Riddle of biofilm resistance. *Antimicrob. Agents Chemother.* **2001**, *45*, 999–1007.
(11) Wilson, B. A.; Smith, V. H.; Denoyelles, F., Jr.; Larive, C. K. Effects of three pharmaceutical mixtures in aquatic microcosms and personal care products on natural freshwater algal assemblages. *Environ. Sci. Technol.* **2003**, *37*, 1713–1719.
(12) Richards, S. M.; Wilson, C. J.; Johnson, D. J.; Castle, D. M.; Lam, M.; Mabury, S. A.; Sibley, P. K.; Solmon, K. R. Effects of pharmaceutical mixtures in aquatic microcosms. *Environ. Toxicol. Chem.* **2004**, *23*, 1035–1042.

(13) Lyman, H. Specific inhibition of chloroplast replication in *Euglena gracilis* by nalidixic acid. *J. Cell Biol.* **1967**, *35*, 726−730.
(14) Krajcovic, J.; Ebringer, L.; Polónyi, J. Quinolones and coumairins eliminate chloroplasts from *Euglena gracilis*. *Antimicrob. Agents Chemother.* **1989**, *33*, 1883–1889.
(15) Wall, M. K.; Mitchenall, L. A.; Maxwell, A. Abaridopsis thaliana DNA gyrase is targeted to chloroplasts and mitochondria. *Proc. Natl. Acad. Sci. U.S.A.* **2004**, *101*, 7821–7826.
(16) Mills, W. R.; Reeves, M.; Fowler, D. L.; Capo, S. F. DNA synthesis in chloroplasts: III. The DNA gyrase inhibitors nalidixic acid and novobiocin inhibit both thymidine incorporation into DNA and photosynthetic oxygen evolution by isolated chloroplasts. *J. Exp. Bot.* **1989**, *40*, 425–429.
(17) Ciarrochi, G.; Nielsen, E.; Cella, R. Effect of nalidixic acid and novobiocin on the metabolism of suspension of cultured carrot cells. *Physiol. Plant* **1985**, *64*, 513–518.
(18) Malkin, R.; Niyogi, K. In *Biochemistry and Molecular Biology of Plants*; Buchanan, B., Gruissem, W., Jones, R., Eds.; American Society of Plant Physiologists: Rockville, MD, 2000; pp 568−628.
(19) Reil, E.; Hofle, G.; Draber, W.; Oettmeier, W. Quinolones and their N-oxides as inhibitors of photosystem II and the cytochrome b_6/f-complex. *Biochim. Biophys. Acta* **2001**, *1506*, 127–132.
(20) Larsson, D. G. J.; de Pedro, C.; Paxeus, N. Effluent from drug manufactures contains extremely high levels of pharmaceuticals. *J. Hazard. Mater.* **2007**, *148*, 751–755.
(21) Roberts, G.; Myatt, G. J.; Johnson, W. P.; Cross, K. P.; Blower, P. E. LeadScope: Software for exploring large sets of screening data. *J. Chem. Inf. Comput. Sci.* **2000**, *40*, 1302–1314.
(22) Aristilde, L. A mechanistic investigation of the environmental chemodynamics of fluoroquinolone antibiotics. Ph.D. dissertation, University of California at Berkeley, 2008; 242 pp.
(23) Goodsell, D. S.; Garrett, M. M.; Olson, A. J. Automated docking of flexible ligands: Applications of autodock. *J. Mol. Recognit.* **1996**, *9*, 1–5.
(24) Morris, G. M.; Goodsell, D. S.; Halliday, R. S.; Huey, R.; Hart, W. E.; Belew, R. K.; Olson, A. J. Automated docking using a Lamarckian genetic algorithm and and empirical binding free energy function. *J. Comput. Chem.* **1998**, *19*, 1639–1662.
(25) Lancaster, C. R. D.; Michel, H. The coupling of light-induced electron transfer and proton uptake as derived from crystal structures of reaction centres from *Rhodopseudomonas viridis* modified at the binding site of the secondary quinone, Q_B. *Structure* **1997**, *5*, 1339–1359.
(26) Zouni, A.; Witt, H.-T.; Kern, J.; Fromme, P.; Krauss, N.; Saenger, W.; Orth, P. Crystal structure of photosystem II from *Synechococcus elongatus* at 3.8 Å resolution. *Nature* **2001**, *409*, 739–743.
(27) *Maestro*, version 7.5; Schrodinger, LLC: New York, 2005.
(28) Hoagland, D. R.; Arnon, D. I. The water-culture method for growing plants without soil. *California Agricultural Experimental Station Circular*; College of Agriculture, University of California: Berkeley, CA, 1950; Vol. 347, p 31.
(29) Melis, A. Functional properties of photosystem II_β in spinach chloroplasts. *Biochim. Biophys. Acta* **1985**, *808*, 334–342.
(30) Bruinsma, J. The quantitative analysis of chlorophylls a and b in plant extracts. *Photochem. Photobiol.* **1963**, *2*, 241–249.
(31) Gleiter, H. M.; Renger, G. In *Target Assays for Modern Herbicides and Related Phytotoxic Compounds*; Boger, P., Gerhard, S., Eds.; Lewis Publishers: Boca Raton, FL, 1993; pp 69−82.
(32) Popovic, R.; Samson, G. Use of algal fluorescence for determination of phytotoxicity of heavy metals and pesticides as environmental pollutants. *Ecotoxicol. Environ. Saf.* **1988**, *16*, 272–278.
(33) Kitajima, M.; Butler, W. L. Quenching of chlorophyll fluorescence and primary photochemistry in chloroplasts by dibromothymoquinone. *Biochim. Biophys. Acta* **1975**, *376*, 105–115.
(34) Melis, A. Regulation of photosystem stoichiometry in oxygenic photosynthesis. *Bot. Mag., Spec. Issue* **1990**, *2*, 9–28.
(35) Brain, R. A.; Ramirex, A. J.; Fulton, B. A.; Chambliss, C. K.; Brooks, B. W. Herbicidal effects of sulfamethoxazole in *Lemna gibba*: Using *p*-aminobenzoic acid as a biomarker of effect. *Environ. Sci. Technol.* **2008**, *42*, 8955–8970.
(36) *SYSTAT Computer Package*, version 13; SYSTAT Inc.: Evanston, IL.
(37) Lancaster, C. R. D.; Michel, H. Refined crystal structures of reaction centres from *Rhodopseudomonas viridis* in complexes with the herbicide atrazine and two chiral atrazine derivatives also lead to a new model of the bound carotenoid. *J. Mol. Biol.* **1999**, *286*, 883–898.
(38) Turiel, E.; Bordin, G.; Rodríguez, A. R. Study of the evolution and degradation products of ciprofloxacin and oxolinic acid in river water samples by HPLC-UV/MS-MS-MS. *J. Environ. Monit.* **2005**, *7*, 189–195.
(39) Brain, R. A.; Hanson, M. L.; Solomon, K. R.; Brooks, B. W. Aquatic plants exposed to pharmaceuticals: Effects and risks. *Res. Environ. Contam. Toxicol.* **2008**, *192*, 67–115.

ES902665N